Kinetic Discrimination between Various Mechanisms in Group-Transfer Polymerization

Axel H. E. Müller

Institut für Physikalische Chemie, Universität Mainz, D-55099 Mainz, Germany

Received October 29, 1993•

ABSTRACT: For various mechanisms of group-transfer polymerization (GTP), the concentration of the active chain ends is calculated. The calculated reaction orders with respect to catalyst and initiator concentrations, respectively, are compared to experimental data for the GTP of methyl methacrylate in THF catalyzed by both bifluoride and benzoate and of *n*-butyl acrylate in toluene catalyzed by mercury iodide. The comparison reveals that for catalysis by benzoate and mercury iodide, the experimental reaction orders are only consistent with the associative mechanism of GTP, i.e., with an activated silyl ketene acetal as the active species. For the catalysis with the less nucleophilic benzoate anion, the existence of a dissociative mechanism (with enolate ions or ion pairs as the active species) can be neither excluded nor proven. The effect of silyl esters which have been used in "livingness enhancers" is discussed and quantified in terms of all mechanisms discussed.

Introduction

As can be judged from some recent reviews,[1-3] the mechanism of group-transfer polymerization (GTP) is presently under dispute. The original "associative" mechanism proposed by Sogah and Webster[4-6] and modified by Mai and Müller[7,8] includes the formation of an active species with pentacoordinate silicon from a silyl ketene acetal and a nucleophilic catalyst Nu^- (e.g., bifluoride or benzoate; Scheme 1). Here, P_i^* and P_i' represent an active and a dormant polymer chain, respectively, with i monomeric units.

Recently, the associative mechanism was questioned by Quirk at al.[2,9,10] It was proposed that enolate ions (or ion pairs) are formed from the silyl ketene acetal and catalyst in a reversible or irreversible reaction ("dissociative mechanism"; Scheme 2). Here, E denotes a trimethylsilyl fluoride or a silyl ester, e.g., trimethylsilyl benzoate. For $K_E \gg 1$, the reaction is irreversible.

Double-labeling experiments were used in order to discriminate between the two mechanisms, since the dissociative mechanism must be accompanied with silyl group exchange. Previous experiments showed fast exchange for difluorotrimethyl siliconate catalysis at room temperature but gave no evidence for exchange with bifluoride catalyst.[5,6] It was argued by others[11,12] that the labels used could potentially change reactivity of the silyl ketene acetals and thus lead to false conclusions. A recent reinvestigation with bifluoride catalyst showed partial exchange.[10] However, it was argued by others[3] that the time needed for the exchange experiment was longer than the time for polymerization. More arguments are given in the reviews mentioned above.[1-3]

Analysis of polymerization kinetics as a function of initial concentrations of reagents can provide a clue for distinguishing between the various possible mechanisms of GTP. A further discrimination is possible by analysis of the molecular weight distributions (MWDs) of the resulting polymers. The latter possibility will be the subject of subsequent publications.[13]

• Abstract published in *Advance ACS Abstracts*, February 15, 1994.

Scheme 1. Associative Mechanism of GTP

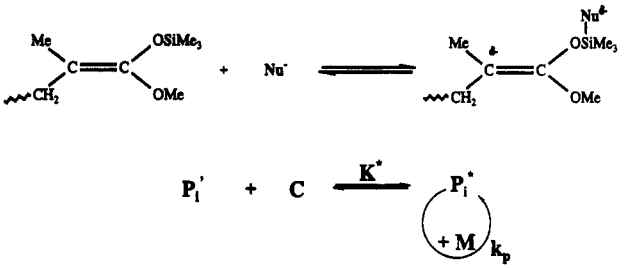

Scheme 2. Dissociative Mechanism of GTP

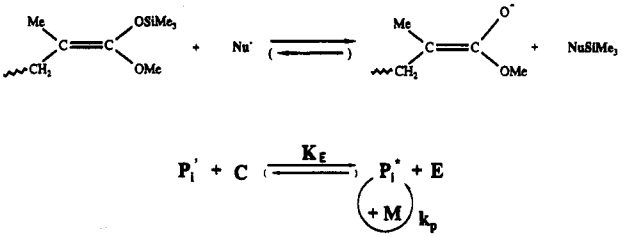

Results and Discussion

Calculation of the Concentration of Active Chain Ends. The rate of polymerization is given by

$$R_p = \frac{dM}{dt} = -k_p M P^* \tag{1}$$

where M and P^* are the concentrations of monomer and active species, respectively, and k_p is the rate constant of propagation. For a living process (i.e., P^* = constant), this leads to the common first-order expression for monomer conversion:

$$\ln \frac{M_0}{M} = k_p P^* t = k_{app} t \tag{2}$$

where the slope of the first-order plot of time vs conversion, $k_{app} = k_p P^*$, is the apparent rate constant.

Since the rate of polymerization is directly proportional to the concentration of active species, P^*, the reaction order with respect to P^* is unity. Assuming that the system is in equilibrium, i.e., P^* = constant, the dependence of

0024-9297/94/2227-1685$04.50/0

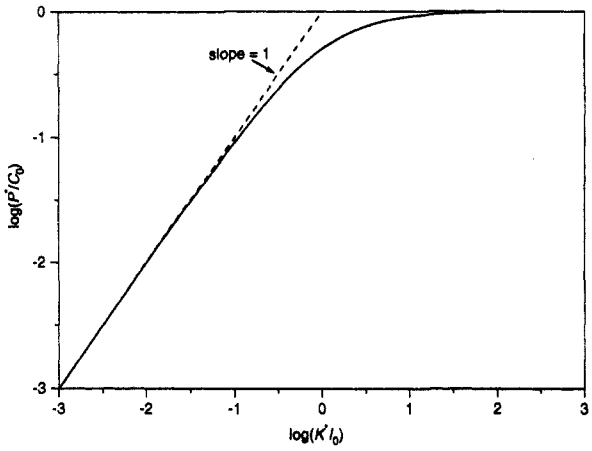

Figure 1. Bilogarithmic plot of the dependence of the concentration of active species, P^*, relative to catalyst concentration, C_0, as a function of K^*I_0 for the associative GTP mechanism (cf. Scheme 1 and eq 5).

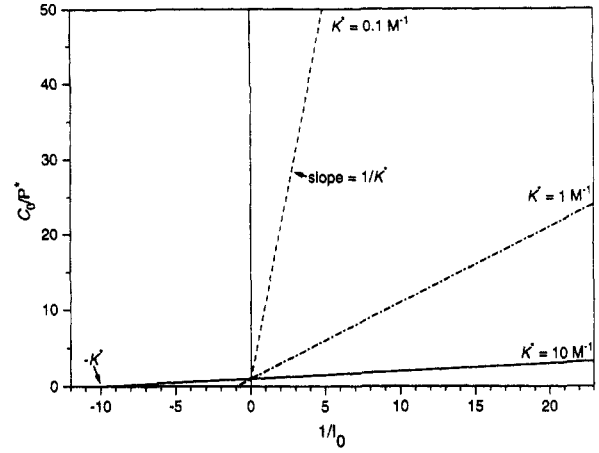

Figure 2. Michaelis–Menten-style treatment of associative mechanism of GTP (cf. eq 7).

P^* on the initial concentrations of catalyst and initiator can be calculated from the mass action law for a certain mechanism. Insertion of the expression for P^* into eq 1 renders the reaction orders for initiator and catalyst which can be compared to experimental data available.

For the ***associative mechanism*** (Scheme 1), the equilibrium constant between dormant and living chain ends is given as

$$K^* = \frac{\sum_i P_i^*}{C\sum_i P_i'} = \frac{P^*}{CP'} \tag{3}$$

where $C = C_0 - P^*$ is the concentration of catalyst and $P' = I_0 - P^*$ is the concentration of dormant polymer chains.

The concentration of active species, P^*, is calculated as

$$P^* = \{[1 + K^*(I_0 + C_0)] - [[1 + K^*(I_0 + C_0)]^2 - 4(K^*)^2 I_0 C_0]^{1/2}\}/2K^* \tag{4}$$

Generally, the concentration of the catalyst is only 0.1–5% of the initiator concentration; i.e., $C_0/I_0 \ll 1$. For this case, we can approximate $P' \approx I_0$. In an earlier paper,[14] P^* was calculated for this case as

$$P^* = \frac{K^*I_0}{1 + K^*I_0} C_0 \tag{5}$$

A bilogarithmic plot of P^*/C_0 vs K^*I_0 is shown in Figure 1. For the limiting case where the equilibrium in Scheme 1 is shifted to the right-hand side, i.e., $K^*I_0 \gg 1$, eq 5 leads to

$$P^* = C_0 \tag{6a}$$

which corresponds to first-order and zero-order kinetics with respect to catalyst and initiator concentrations, respectively. Figure 1 shows that within experimental error, the condition is fulfilled for $K^*I_0 \geq 10$.

If the equilibrium is shifted to the left-hand side, i.e., $K^*I_0 \ll 1$, this leads to

$$P^* = K^*I_0C_0 \tag{6b}$$

which corresponds to first-order kinetics with respect to both catalyst and initiator concentrations. Figure 1 shows that the condition is approximately fulfilled for $K^*I_0 \leq 0.1$.

For the intermediate region, i.e., $K^*I_0 \approx 1$, the kinetic order with respect to initiator concentration is fractional. Interestingly, the formation of active chain ends from catalyst and dormant chain ends is kinetically identical to the formation of an enzyme–substrate complex, where catalyst and initiator correspond to enzyme and substrate, respectively. Accordingly, Michaelis–Menten kinetics[15] can be applied, where K^* corresponds to the reciprocal Michaelis–Menten constant, $1/K_M$. Linearization of eq 5 renders (Figure 2)

$$\frac{1}{P^*} = \frac{1}{C_0} + \frac{1}{C_0K^*}\frac{1}{I_0} \tag{7}$$

Combination with eq 2 leads to a Lineweaver–Burk plot:

$$\frac{1}{k_{app}} = \frac{1}{k_pC_0} + \frac{1}{k_pC_0K^*}\frac{1}{I_0} \tag{8}$$

By plotting $1/k_{app}$ vs $1/I_0$, the values of K^* and k_p can be determined from the intercept of the straight line with the abscissa and the ordinate, respectively. A similar relation was recently given by Bywater.[1] By rearrangement of eq 8, one obtains an Eadie–Hofstee plot which allows for a better detection of nonlinearity:

$$k_{app} = k_pC_0 - \frac{k_{app}}{K^*}\frac{1}{I_0} \tag{8a}$$

For the ***reversible dissociative mechanism*** (Scheme 2), the equilibrium constant for enolization, K_E, is given by

$$K_E = \frac{E\sum_i P_i^*}{C\sum_i P_i'} = \frac{EP^*}{CP'} = \frac{(P^*)^2}{CP'} \tag{9}$$

The concentration of active species is calculated as

$$P^* = \{K_E(I_0 + C_0) - [[K_E(I_0 + C_0)]^2 - 4K_E(K_E - 1)I_0C_0]^{1/2}\}/2(K_E - 1) \tag{10}$$

For $C_0/I_0 \ll 1$, eq 10 simplifies to

$$P^* = \frac{K_E I_0}{2}\left(-1 + \left[1 + \frac{4C_0}{K_E I_0}\right]^{1/2}\right) \quad (11)$$

The dependence of P^* on I_0 and C_0 is shown in Figures 3 and 4, respectively. For the limiting case $K_E I_0 \ll C_0$, eq 11 leads to

$$P^* = (K_E I_0 C_0)^{1/2} \quad (12a)$$

which corresponds to half-order kinetics with respect to both catalyst and initiator concentrations. For $K_E I_0 \gg C_0$, we can expand eq 11 into a Taylor series and neglect higher than linear terms which leads to

$$P^* = C_0 \quad (12b)$$

This corresponds to first-order and zero-order kinetics with respect to catalyst and initiator concentrations, respectively.

For the ***irreversible dissociative mechanism*** (corresponding to $K_E \gg 1$), the concentration of active species is identical to the case described by eq 12b.

Effect of Complexation of Enolate with Silyl Ketene Acetal. In the case of the dissociative mechanisms, the free enolate may be stabilized by formation of a complex with "dormant" silyl ketene acetals (cf. Scheme 3). This complex presumably is also inactive.

The equilibrium constant for complex formation, K_c, is given by

$$K_c = \frac{(P^*P')}{P^*P'} \approx \frac{(P^*P')}{P^*I_0} \quad (13)$$

For the ***reversible dissociative mechanism***, eq 9 has to be modified since $P^* < E$. Combination of eqs 9 and 13, introduction of the new mass balances

$$I_0 = P' + P^* + (P^*P') \approx P'$$

$$C_0 = C + P^* + (P^*P')$$

$$E = P^* + (P^*P')$$

and taking into account that $P^* \ll I_0$ and $(P^*P') \ll I_0$ lead to

$$K_E = \frac{P^*(P^* + K_c P^* I_0)}{I_0(C_0 - P^* - K_c P^* I_0)} \quad (14)$$

and

$$P^* = \frac{K_E I_0}{2}\left(-1 + \left[1 + \frac{4C_0}{(1 + K_c I_0)K_E I_0}\right]^{1/2}\right) \quad (15)$$

Some examples of this relation are given in Figure 5 for $C_0 = 10^{-6}$ M, $K_c = 10^3$ M, and various values of K_E. The limiting case that the complexation equilibrium (Scheme 3) is shifted to the left-hand side (i.e., $K_c I_0 \ll 1$) obviously leads to eq 11. The opposite case ($K_c I_0 \gg 1$) leads to

$$P^* = \frac{K_E I_0}{2}\left(-1 + \left[1 + \frac{4C_0}{K_c K_E I_0^2}\right]^{1/2}\right) \quad (16)$$

Here, again, two limiting cases can be discussed. For $K_c K_E I_0^2 \ll C_0$ (i.e., equilibrium of Scheme 2 shifted to the left-hand side),

$$P^* = \frac{C_0}{I_0} \quad (17a)$$

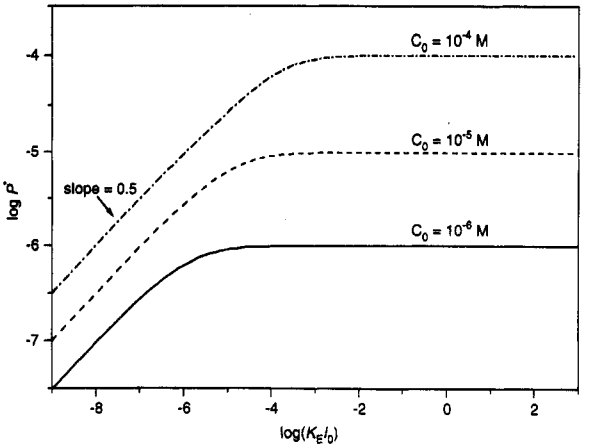

Figure 3. Bilogarithmic plot of the dependence of the concentration of active species, P^*, as a function of $K_E I_0$ for the reversible dissociative GTP mechanism (cf. Scheme 2 and eq 11).

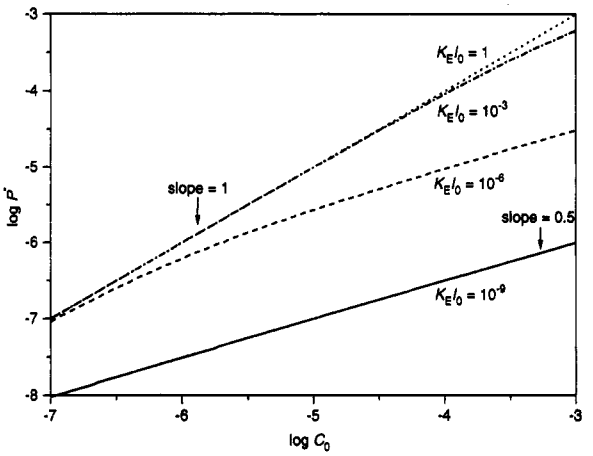

Figure 4. Bilogarithmic plot of the dependence of the concentration of active species, P^*, as a function of C_0 for the reversible dissociative GTP mechanism (cf. Scheme 2 and eq 11).

and for $K_c K_E I_0^2 \gg C_0$,

$$P^* = \left(\frac{C_0 K_E}{K_c}\right)^{1/2} \quad (17b)$$

Thus, the reaction order with respect to catalyst concentration remains unchanged, i.e., lies in the range 0.5...1, whereas the reaction order with respect to initiator concentration is changed; it lies in the range −1...0. This means that the initiator (and the dormant chain ends) acts as an inhibitor. If the complex should have some remaining activity, the true reaction orders will lie in between the extreme cases of eqs 12a,b and 17a,b.

For the ***irreversible dissociative mechanism***, the concentration of active chains is given by

$$P^* = \frac{C_0}{1 + K_c I_0} \quad (18)$$

which leads to

$$P^* = \frac{C_0}{K_c I_0} \quad (19a)$$

for $K_c I_0 \gg 1$ and

$$P^* = C_0 \quad (19b)$$

for $K_c I_0 \ll 1$. Again, the reaction order for catalyst remains unchanged at unity, whereas the reaction order for initiator is decreased by one.

Scheme 3. Stabilization of Enolates by Silyl Ketene Acetals

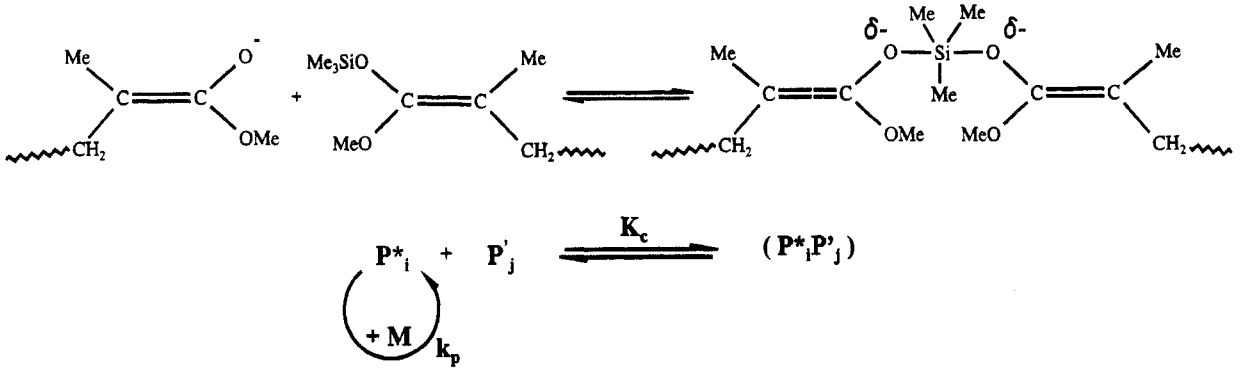

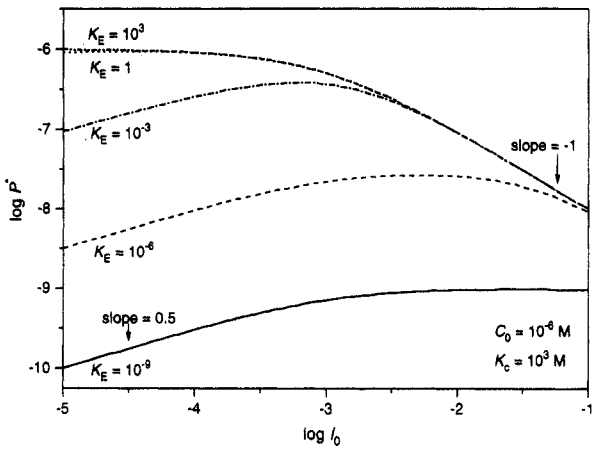

Figure 5. Bilogarithmic plot of the dependence of the concentration of active species, P^*, as a function of I_0 for the reversible dissociative GTP mechanism including complexation of enolate with silyl ketene acetal (cf. Scheme 3 and eq 15).

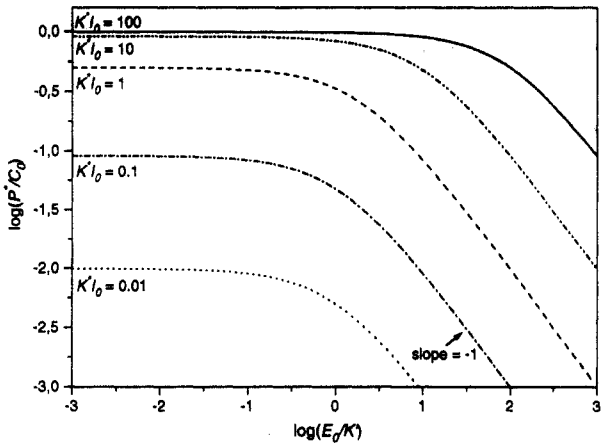

Figure 6. Bilogarithmic plot of active center concentration, P^*, vs the initial concentration of added silyl ester, E_0 (competitive inhibition, cf. eq 20).

Scheme 4. Competitive Inhibition by Silyl Esters (E)

$$P_i^{\cdot} + C \overset{K^*}{\rightleftharpoons} P_i^*$$

$$E + C \overset{K'}{\rightleftharpoons} E^*$$

Effect of Livingness Enhancers. It was reported that trimethylsilyl esters can act as "livingness enhancers".[16] This effect may be understood in terms of both mechanisms.

With regard to the ***associative mechanism***, the stabilizing effect of silyl esters can be attributed to their potential to compete with silyl ketene acetals for coordination with catalyst (Scheme 4). This competition

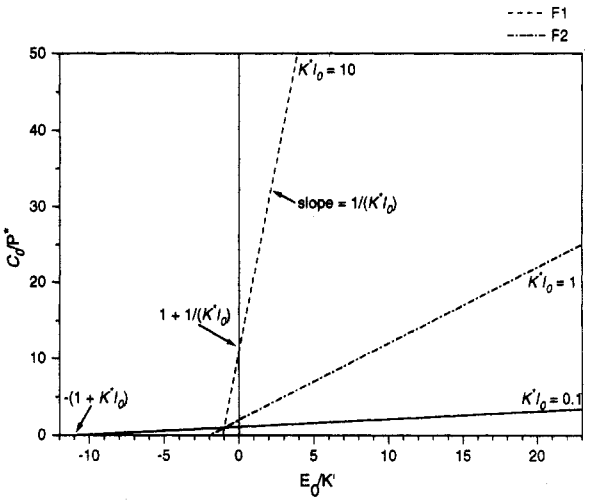

Figure 7. Michealis–Menten-style plot for competitive inhibition by added silyl ester, E_0, according to eq 21.

decreases the fraction of active chains and thus the rates of both termination and propagation. The effect is identical to competitive inhibition in enzyme kinetics, and in analogy to the Michaelis–Menten treatment (with E as the inhibitor), the concentration of active centers is calculated by modifying eq 5:[15]

$$P^* = \frac{K^* I_0 C_0}{1 + K^* I_0 + \dfrac{E_0}{K'}} \tag{20}$$

Here, $E_0 = E + E^*$ corresponds to the initial concentration of added ester and K' is the equilibrium constant for addition of catalyst to the silyl group of the ester (corresponding to the reciprocal inhibition constant in Michaelis–Menten kinetics). Some examples are given in Figure 6. Linearization according to the Michaelis–Menten treatment leads to (Figure 7)

$$\frac{C_0}{P^*} = 1 + \frac{1}{K^* I_0} + \frac{1}{K^* I_0 K'} E_0 \tag{21}$$

Combination of eq 21 with eq 2 leads to the Lineweaver–Burk and Eadie–Hofstee plots, respectively:

$$\frac{1}{k_{app}} = \frac{1}{k_p C_0} + \frac{1}{k_p C_0 K^* I_0} + \frac{1}{k_p C_0 K^* K' I_0} E_0 \tag{21a}$$

$$k_{app} = k_p C_0 - \frac{k_{app}}{K^* I_0} - \frac{k_{app}}{K' K^* I_0} E_0 \tag{21b}$$

Figure 6 shows that the reaction order with respect to ester concentration (cf. eq 20) is fractional. However, we

can again determine the limiting cases. For $E_0/K' \ll 1$, the reaction order obviously is 0, whereas for $E_0/K' \gg 1$, eq 21 leads to

$$k_{app} = \frac{k_p K^* K' C_0 I_0}{E_0} \quad (22)$$

which corresponds to a reaction order of −1 with respect to E_0.

With regard to the ***reversible dissociative mechanism***, the effect of livingness enhancers is easily understood from Scheme 2, i.e., by decreasing the fraction of active chain ends. The concentration of free ester is $E = E_0 + P^*$, and the concentration of active species is calculated as

$$P^* = \{K_E(I_0 + C_0) + E_0 - [[K(I_0 + C_0) + E_0]^2 - 4K_E(K_E - 1)I_0C_0]^{1/2}\}/2(K_E - 1) \quad (23)$$

For $C_0/I_0 \ll 1$, eq 10 leads to

$$P^* = \frac{E_0 + K_E I_0}{2} + \frac{1}{2}[(E_0 + K_E I_0)^2 + 4C_0 K_E I_0]^{1/2} \quad (24)$$

The dependence of P^* on E_0 is also nonlinear. Again, the limiting cases can be calculated. For $E_0 \ll K_E I_0$, the reaction order again is 0, and for $E_0 \gg K_E I_0$, the dependence of P^* on E_0 is given by

$$P^* = \frac{C_0 K_E I_0}{E_0} \quad (25)$$

which again leads to a reaction order of −1 for E_0.

For the ***irreversible dissociative mechanism***, addition of esters should have no effect unless the structure of the acid residue strongly differs from that of the catalyst anion.

Comparison with Experimental Reaction Orders. By comparing eqs 6, 12, and 19, we see that the kinetic order of GTP with respect to catalyst and initiator concentrations depends on the mechanism and on the magnitude of the equilibrium constants K^* or K_E and K_c. In Table 1, the calculated reaction orders are compared

Table 1. Theoretical and Experimental Reaction Orders with Respect To Catalyst and Initiator Concentrations for Group-Transfer Polymerization of Methyl Methacrylate (MMA) and *n*-Butyl Acrylate (nBuA)

mechanism	C_0[f] calcd	I_0[g] calcd
associative	1	0...1
reversible dissociative	1/2...1	0...1/2
reversible dissociative w/complexation[a]	1/2...1	−1...1/2
irreversible dissociative	1	0
irreversible dissociative w/complexation[a]	1	−1...0

monomer/catalyst/solvent	C_0 exptl	I_0 exptl
MMA/TAS[b] bifluoride/THF	1.17[c,14]	0[8]
MMA/TAS[b] benzoate/THF	0.9[7,17]	1.2[7]
		0.7[d,18]
nBuA/HgI_2/toluene[19]	0.94	1.25
	1.2[e]	0.7[e]

[a] Taking into account the formation of an inactive complex of enolate with silyl ketene acetal (eqs 17 and 19). [b] TAS = tris(dimethylamino)sulfonium. [c] For *initiation*, the reaction order was found to be 2.[17] This was accounted for by assuming a preequilibrium between bifluoride and fluoride anions. [d] "Dimeric" initiator methyl 5-methoxy-2,2,4-trimethyl-5-(trimethylsiloxy)-4-pentenoate. [e] In the presence of trimethyl silyl iodide. [f] Reaction order for catalyst concentration. [g] Reaction order for initiator concentration.

Scheme 5. Direct Activity Exchange between Living and Dormant Chain Ends

$$P_i^* + P_j' \rightleftharpoons P_i' + P_j^*$$

to the experimental data available for the GTP of methyl methacrylate in THF and *n*-butyl acrylate in toluene.

Table 1 shows that the experimental data for bifluoride catalysis are consistent with all three mechanisms, given the equilibrium is shifted to the right-hand side. On the contrary, *for catalysis by benzoate or HgI_2/trimethylsilyl iodide, the experimental data are only consistent with the associative mechanism.* Thus, at least *for bifluoride catalysis, further discrimination is needed.* This may be obtained by comparing the actual dependence of k_{app} on I_0 and C_0 over a larger range of concentrations. However, since for bifluoride catalysis the equilibrium for both Scheme 1 and Scheme 2 appears to be shifted to the right-hand side, the precision of data is not sufficient for a distinction between the mechanisms according to eqs 8, 8a, and 11.

A further discrimination can be obtained from livingness enhancer experiments: they can be used to directly differentiate between the reversible and the irreversible dissociative mechanisms. Associative and reversible dissociative mechanisms cannot be directly distinguished from the reaction order with respect to ester concentration but from the actual dependence of rate on E_0 which follows different laws. Unfortunately, there are no kinetic data available at this moment.

An additional problem has to be addressed: since the fraction of active chain ends is much smaller than the total number of polymer chains, activity exchange between the active and dormant chain ends is necessary in order for all the chains to grow. Besides the indirect mechanisms of activity exchange given in Scheme 1, i.e., by dissociation/association of catalyst, or in Scheme 2, i.e., by silylation/enolization, a direct exchange between living and dormant chain ends is also feasible (Scheme 5). For the associative mechanism, this means direct transfer of catalyst between an activated and a nonactivated silyl ketene acetal. For the dissociative mechanism, this means transfer of a trimethylsilyl group from a "dormant" silyl ketene acetal to an active enolate chain end and is equivalent to Scheme 3. Since the total concentration of active chain ends remains constant, kinetic measurements do not allow for discrimination between indirect and direct activity exchange. Only for the irreversible dissociative mechanism is this the only possibility of exchange activity between chain ends. Information about the activity exchange mechanism as well as a further distinction of associative and dissociative mechanisms may be obtained from MWD data.[13]

Acknowledgment. This work was supported by the Deutsche Forschungsgemeinschaft within the Sonderforschungsbereich 262 "Nichtmetallische amorphe Materialien".

References and Notes

(1) Bywater, S. *Makromol. Chem.; Macromol. Symp.* **1993**, *67*, 339.
(2) Quirk, R. P.; Ren, J.; Bidinger, G. *Makromol. Chem.; Macromol. Symp.* **1993**, *67*, 351.
(3) Webster, O. W. *Makromol. Chem.; Macromol. Symp.* **1993**, *67*, 365.
(4) Webster, O. W.; Hertler, W. R.; Sogah, D. Y.; Farnham, W. B.; RajanBabu, T. V. *J. Am. Chem. Soc.* **1983**, *105*, 5706.
(5) Sogah, D. Y.; Farnham, W. B. In *Organosilicon and Bioorganosilicon Chemistry*; Sakurai, H., Ed.; Wiley: New York, 1986; p 219.

(6) Farnham, W. B.; Sogah, D. Y. *Polym. Prepr., Am. Chem. Soc., Div. Polym. Chem.* **1986**, *27* (1), 167.
(7) Müller, A. H. E. *Makromol. Chem., Macromol. Symp.* **1990**, *32*, 87.
(8) Mai, P. M.; Müller, A. H. E. *Makromol. Chem., Rapid Commun.* **1987**, *8*, 247.
(9) Quirk, R. P.; Bidinger, G. P. *Polymer Bull. (Berlin)* **1989**, *22*, 63.
(10) Quirk, R. P.; Ren, J. *Macromolecules* **1992**, *25*, 6612.
(11) Matyjaszewski, K. *New Polym. Mater.* **1990**, *2*, 115.
(12) Martin, D. T.; Bywater, S. *Makromol. Chem.* **1992**, *193*, 1011.
(13) Müller, A. H. E.; Zhuang, R.; Yan, D. Y. To be submitted to *Macromolecules*.
(14) Mai, P. M.; Müller, A. H. E. *Makromol. Chem., Rapid Commun.* **1987**, *8*, 99.
(15) Lehninger, A. L. *Biochemie*, 2nd ed.; VCH: Weinheim, 1977.
(16) Schneider, L. V.; Dicker, I. B. Eur. Pat. Appl. EP 244953, to E. I. du Pont de Nemours & Co., 1987; *Chem. Abstr. 108*, 205280.
(17) Brittain, W. J. *J. Am. Chem. Soc.* **1988**, *110*, 7440.
(18) Hofe, T. Diplomarbeit, Mainz, 1990.
(19) Zhuang, R.; Müller, A. H. E. *Abstr., EPF Workshop Anionic Polym. Rel. Process., Mainz* **1992**, *74*.